ADVANCED FUNCTIONAL MATERIALS

Supporting Information

for *Adv. Funct. Mater.*, DOI: 10.1002/adfm.201908349

Void-Free 3D Bioprinting for In Situ Endothelialization and Microfluidic Perfusion

*Liliang Ouyang, James P. K. Armstrong, Qu Chen, Yiyang Lin, and Molly M. Stevens**

Supporting information

Void-free 3D Bioprinting for In-situ Endothelialization and Microfluidic Perfusion

*Liliang Ouyang, James P. K. Armstrong, Qu Chen, Yiyang Lin and Molly M. Stevens**

*Corresponding author. Email: m.stevens@imperial.ac.uk

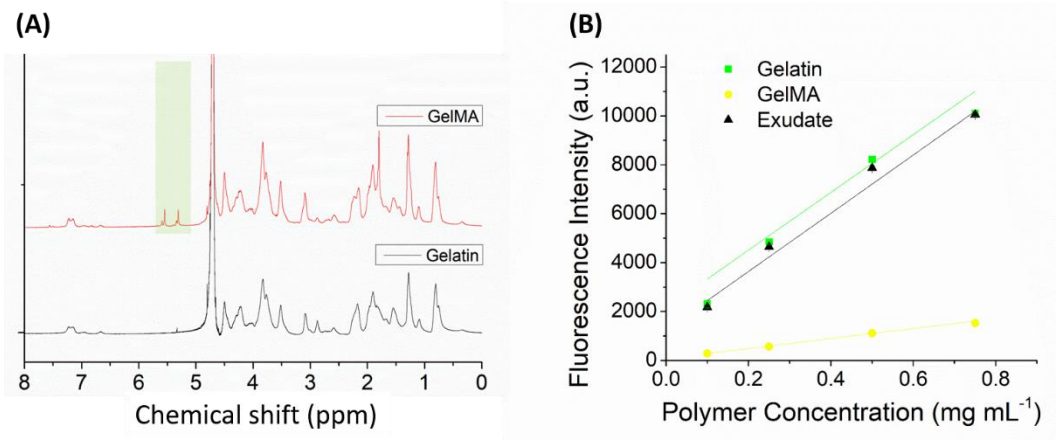

Figure S1. Degree of modification measurements and assessment of exudate. (A) ^{1}H-NMR spectra of gelatin (black trace) and GelMA (red trace) indicating the successful conjugation of methacrylate groups (green shade). (B) Quantitative assessment from a fluoraldehyde assay indicating gelatin standards (green markers and linear fit), GelMA (yellow markers and linear fit) and the exudate (black markers and linear fit). The exudate was measured from the lyophilized liquid exuded from a VF-3DP construct after 30 min incubation at 37 °C.

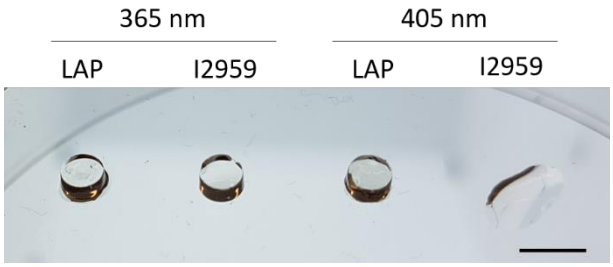

Figure S2. Photo-crosslinking of 7.5 wt% GelMA containing either 0.05 wt% LAP or 0.05 wt% I2959 under either UV (365 nm, ~5 mW cm^{-2}) or blue light (405 nm, ~0.1 W cm^{-2}) irradiation for 5 min. The gel was cast in a 0.5 mL syringe with 20 µl volume. Scale bar: 5 mm.

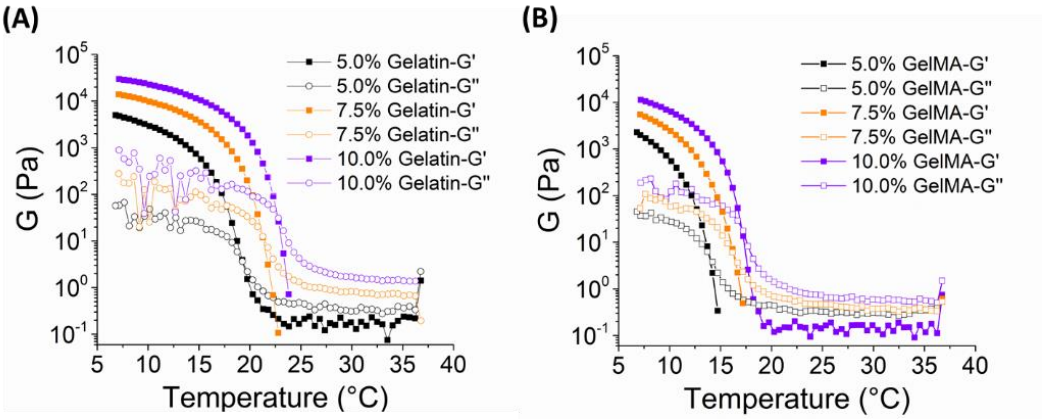

Figure S3. Rheological characterization. Representative curves of the storage (G') and loss (G'') components of the shear modulus (G) were measured for (A) gelatin and (B) GelMA at different concentrations under temperature sweep (cooling at 5 °C min^{-1}).

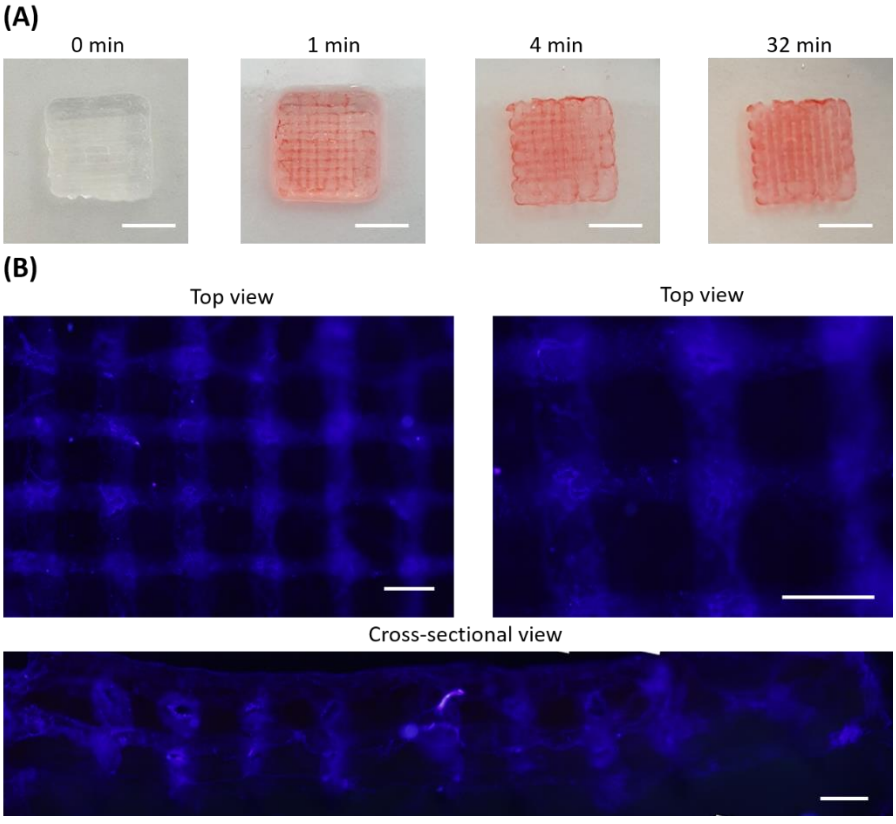

Figure S4. Interconnection of generated channels. (A) Snapshots from Movie S2 showing uptake of dye solution (red) into a VF-3DP lattice. (B) Top and cross-sectional views of the structure after soaking with fluorescence beads (blue), which could be used to demarcate the lumen. Scale bars: 5 mm (A), 500 μm (B).

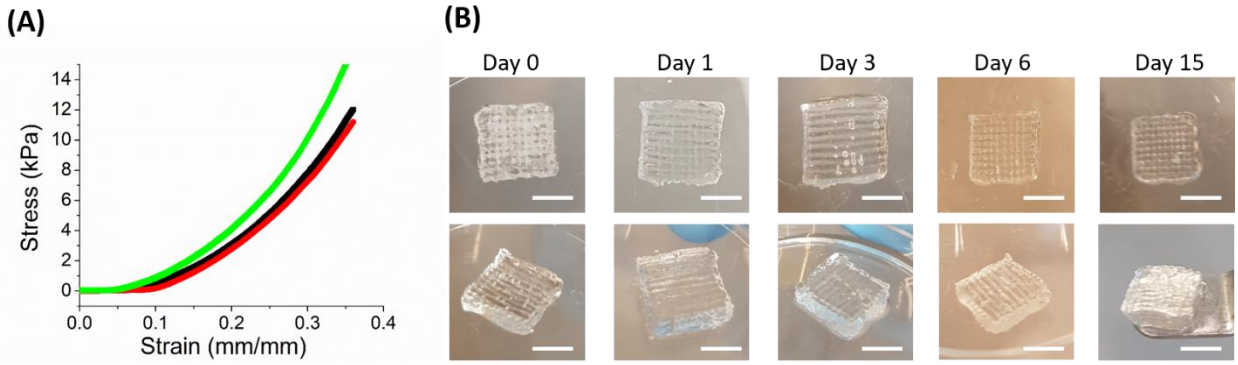

Figure S5. Mechanical stability of VF-3DP structure. (A) Representative stress-strain curve of three sample replicates with compression test (0.01 mm s^{-1} ramp rate) performed at day 1. (B) Stability of the VF-3DP final structure during incubation in PBS (37 ° C) for up to 15 days, indicating maintenance of the structural integrity and channel features. Scale bars: 5 mm.

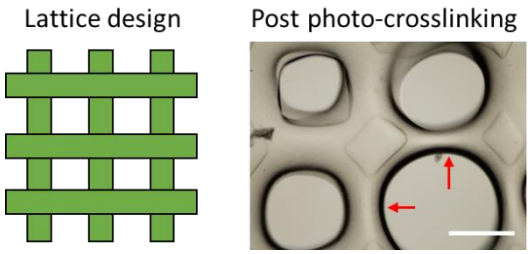

Figure S6. Representative image of the lattice structure formed after photo-crosslinking a directly printed 7.5 wt% GelMA. Arrows indicate large, expanded pores that were not observed in the VF-3DP. Scale bar: 500 μm.

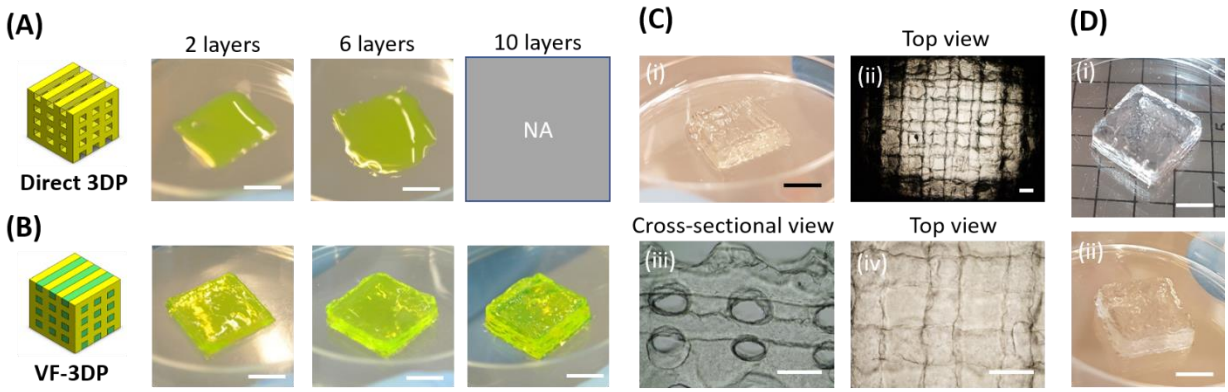

Figure S7. Enhanced printability using VF-3DP. (A) Direct 3D printing and (B) VF-3DP of low concentration GelMA (5 wt%) in a typical layer-by-layer fashion (yellow color indicates GelMA supplemented with fluorescein). The direct 3D printing could not support any stable structures, even after just two layers. (C) Representative images of VF-3DP 5 wt% GelMA structures with top and cross-sectional views, showing the interconnected channels. (D) Generalization of the VF-3DP approach for printing (i) 5 wt% MeHA and (ii) 5 wt% NorHA. Scale bars: 5 mm (A, B, C(i), D), 500 μm (C(ii-iv)).

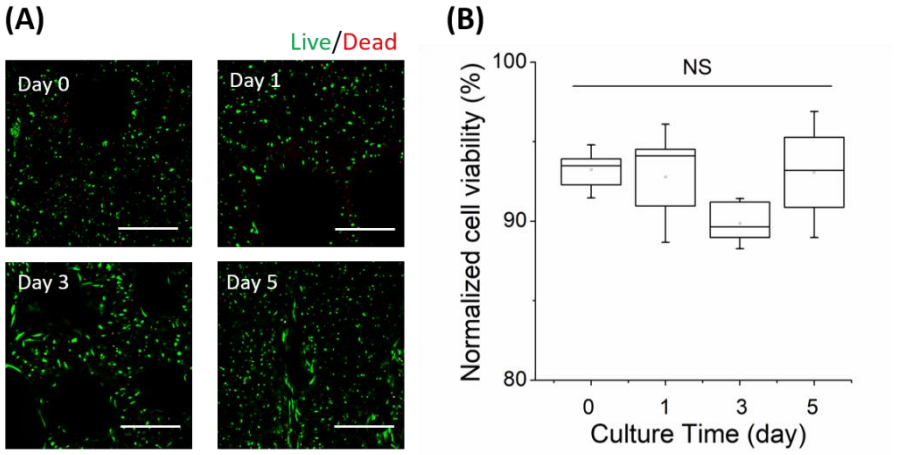

Figure S8. Cell viability post-printing. (A) Representative LIVE/DEAD™ staining images of VF-3DP of 7.5 wt% GelMA embedded with HDF cells (5×10^6 cells mL^{-1}). The majority of cells were viable (green) with only a small proportion of nonviable cells (red). (B) Image analysis was used to quantify cell viability over 5 d of culture. Scale bars: 500 μm. Data shown as mean ± standard deviation, $n \geq 4$, NS = nonsignificant (Kruskal-Wallis unmatched test).

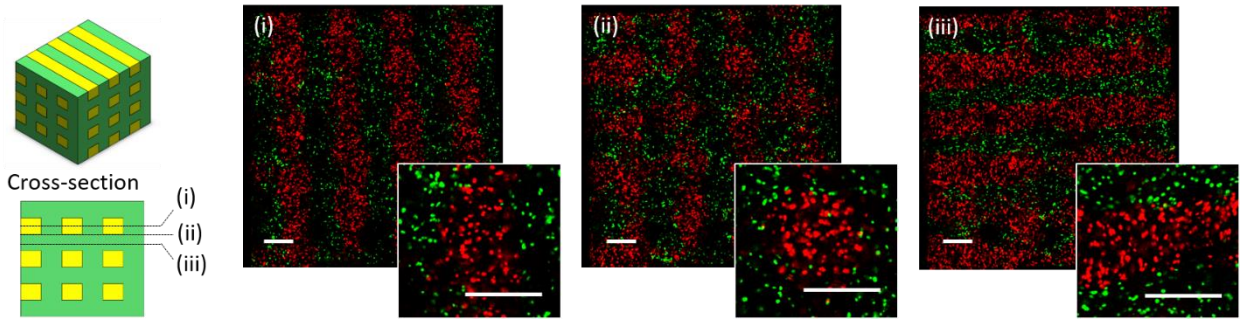

Figure S9. Representative confocal fluorescence microscopy images of a VF-3DP construct seeded with two different cell types. Each image set (i, ii, iii) shows the cell distribution at different levels. HUVECs stained with cell tracker (red, Alexa Fluor™ 647) were in the 7.5 wt% gelatin bioink while HDFs stained with cell tracker (green, Alexa Fluor™ 488) were in the 7.5 wt% GelMA bioink. Both bioinks contained 5×10^6 cells mL^{-1}. Scale bars: 500 μm.

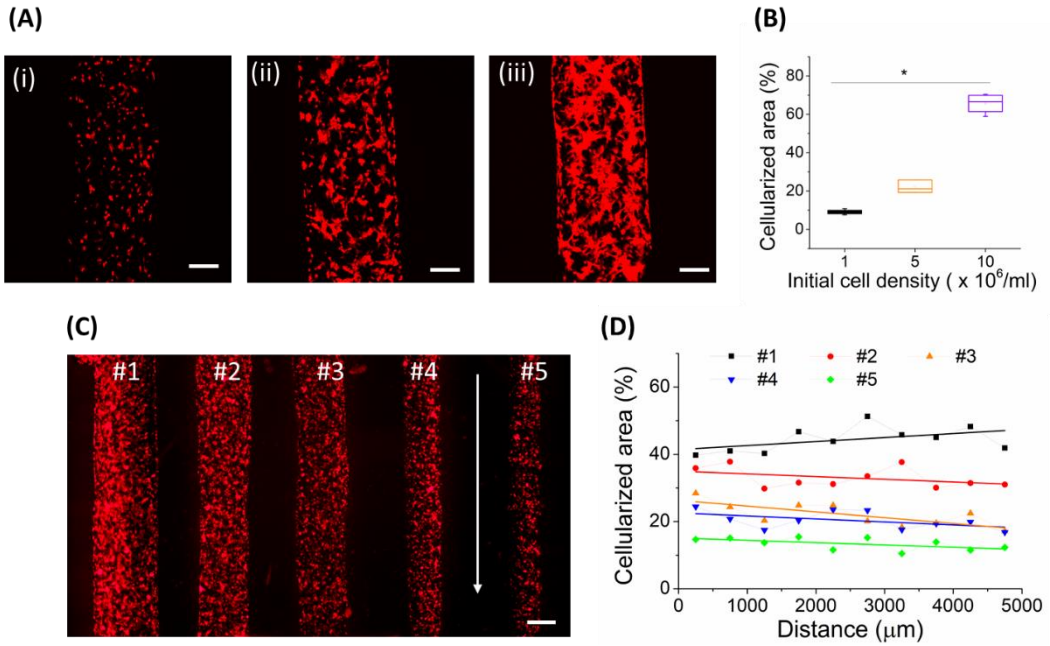

Figure S10. (A) Confocal fluorescence microscopy images of in-situ seeded RFP-labeled HUVECs after culturing for 6 h, with initial cell concentration of (i) 1×10^6, (ii) 5×10^6, and (iii) 10×10^6 cells per mL. (B) Cell occupation in the channel was quantified by estimating the fluorescence area ratio. Data shown as mean ± standard deviation from four samples (one-tailed Mann–Whitney test), $p \leq 0.05$ (*). (C) Fluorescence images of in-situ seeded RFP-labeled HUVECs (initial cell concentration of 5×10^6 cells per mL) in channels of varied sizes and (D)

the corresponding cellularized area profile along the longitudinal axis of the channels. The white arrow indicates the profile direction. Scale bars: 200 μm (A), 500 μm (C).

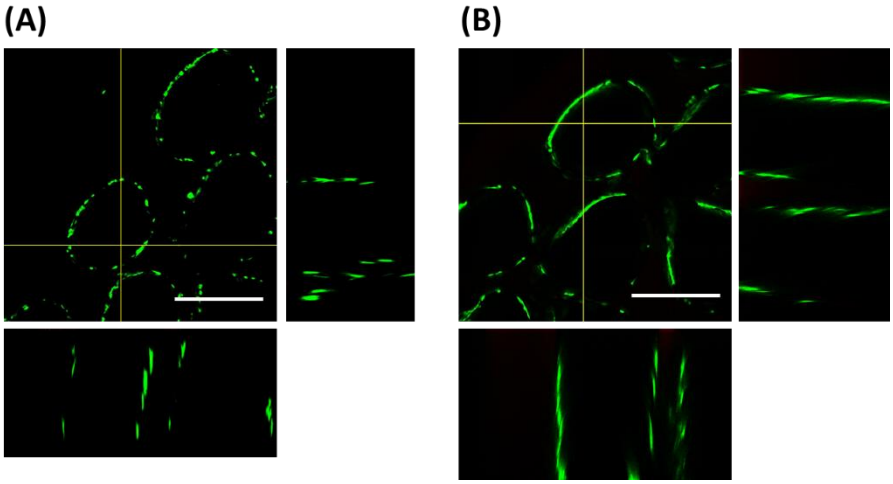

Figure S11. Confocal fluorescence microscopy images of cross-sectional cell-laden constructs with parallel channel design at (A) day 1 and (B) day 3, indicating the distribution of LIVE/DEAD™ stained cells (live cells: green, dead cells: red) on the channel walls. Scale bars: 500 μm.

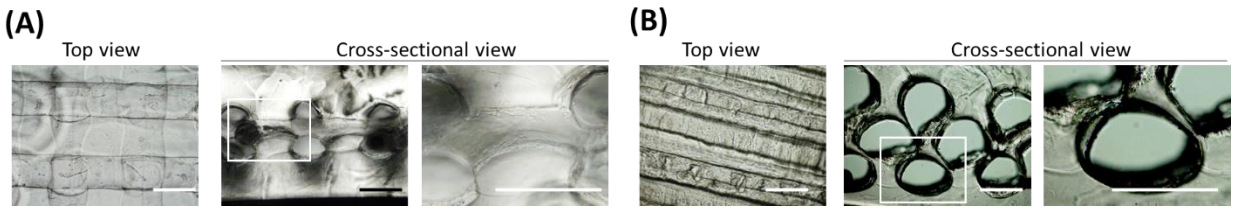

Figure S12. Representative images of HUVEC-laden 3D contructs captured at day 3 showing both the top and cross-sectional views of the (A) lattice and (B) parallel designs. Scale bars: 500 μm.

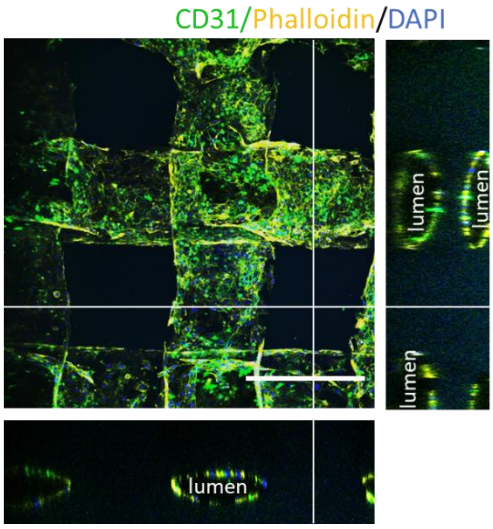

Figure S13. Confocal fluorescence microscopy images of immunostained constructs at day 8 indicated full occupation of CD31-positive HUVECs. Scale bar: 500 µm.

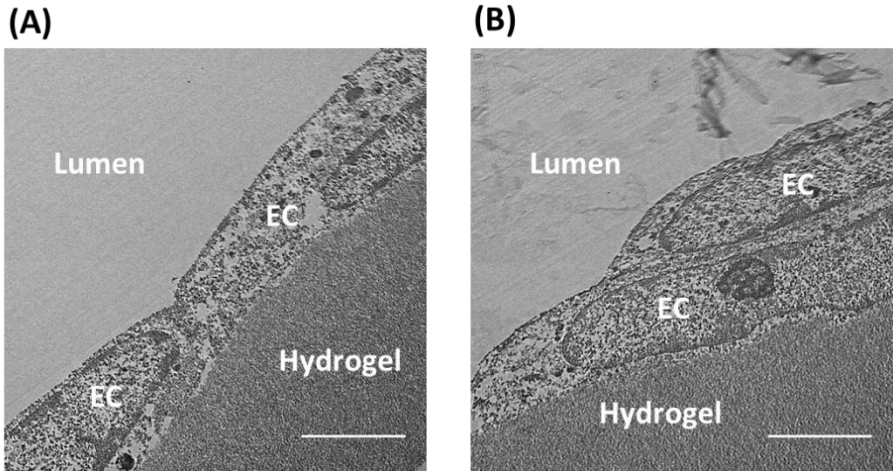

Figure S14. Transmission electron micrographs of the hydrogel-lumen interface. (A) focal contacts and (B) overlapping junctions between endothelial cells (EC). Scale bars: 2 µm.

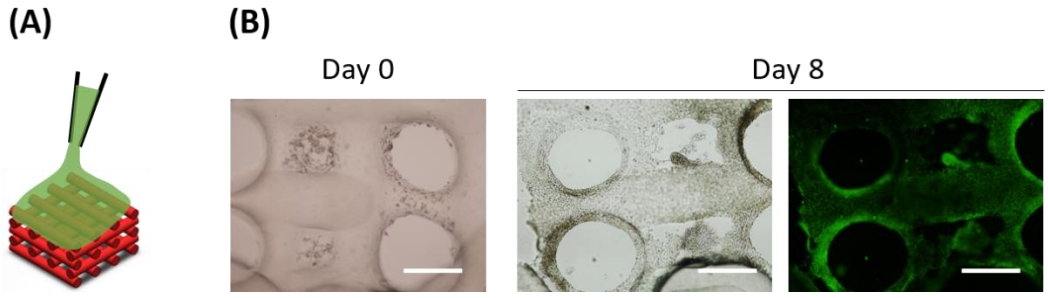

Figure S15. (A) Schematic of seeding cells on a directly-printed porous lattice scaffold. (B) Representative bright field microscopy and fluorescence microscopy images of the directly-printed GelMA (7.5 wt%) structure taken 0 and 8 d after HUVEC seeding. The HUVECs were stained using calcein-AM (green). Scale bars: 500 μm.

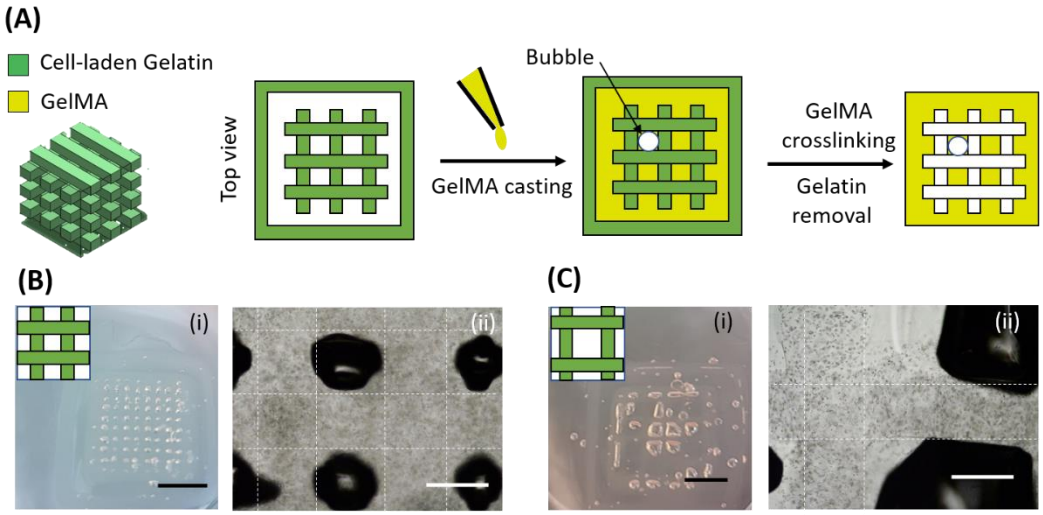

Figure S16. Post-casting approach for porous structure fabrication. (A) Schematic of the fabrication process, where HUVEC-laden gelatin (7.5 wt%) was directly printed into porous lattice structure and then GelMA (7.5 wt%) solution was added slowly onto the structure, aiming to fill up the porous space. After crosslinking GelMA and dissolving gelatin, defective matrix casting was observed by photography and bright field microscopy. This was observed for structures cast with (B) 1 mm and (C) 2 mm distance between gelatin filaments. The defective casting appeared to arise from bubbles generated in the lattice pores. Scale bars: 5 mm (B(i), C(i)), 500 μm (B(ii), C(ii)).

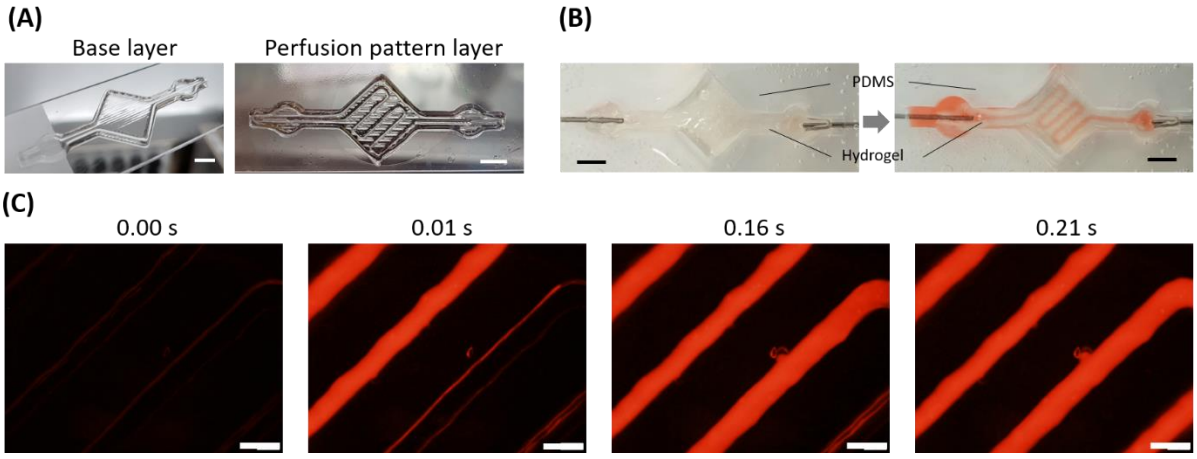

Figure S17. Hydrogel-based microfluidics. (A) Representative photographs of the printed base layer and perfusion pattern. (B) Photographs showing the hydrogel device integrated with a PDMS set-up for peristaltic perfusion and (C) fluorescence microscopy images showing the perfusion of rhodamine solution. Scale bars: 5 mm (A, B), 500 μm (C).

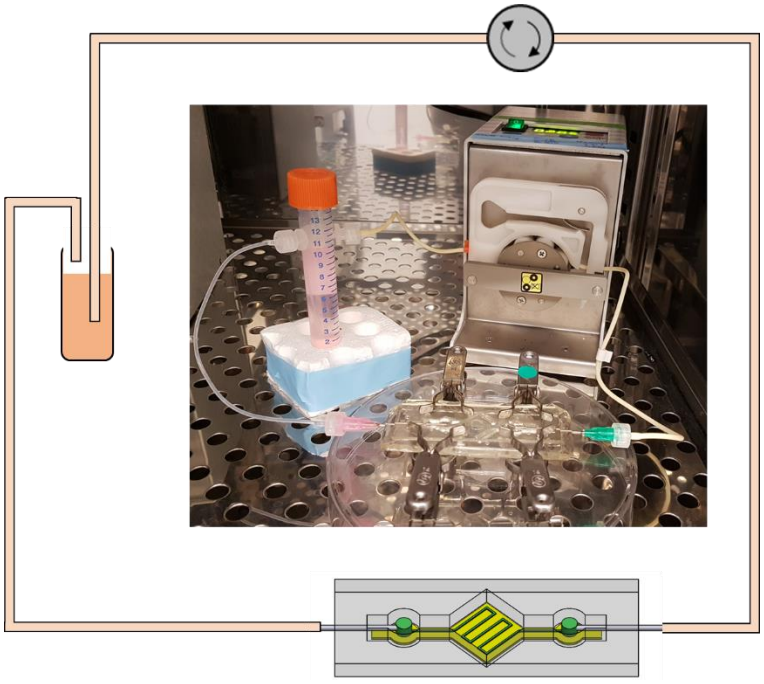

Figure S18. Perfusion culture set-up containing a cellularized hydrogel-based device (bottom), a peristaltic pump (top) and a medium reservoir (left) in circulation.

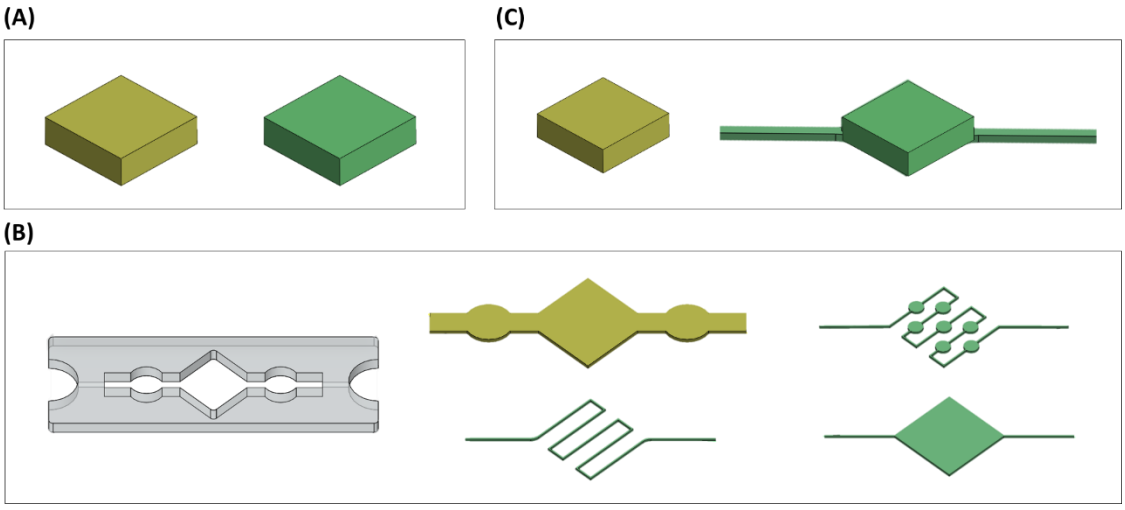

Figure S19. CAD models used for (A) typical VF-3DP, (B) hydrogel microfluidics interfaced with a PDMS casing (grey) and (C) self-standing hydrogel microfluidics. Matrix bioink (yellow) and templating bioink (green) were assigned to the corresponding parts during printing. VF-3DP was performed by defining the infill patterns of two parts to be complementary.

Supplementary Movies

Movie S1. VF-3DP process using two bioinks (7.5 wt% gelatin and 7.5 wt% GelMA).

Movie S2. Demonstration of interconnected channels by dripping dye solution onto the VF-3DP structure (10 × 10 × 3 mm).

Movie S3. Confocal fluorescence microscopy 3D view of in-situ seeded RFP-labeled HUVECs in the channel at day 0.

Movie S4. Confocal fluorescence microscopy z-stack at day 8 showing the alignment of HUVECs on the walls of the interconnected channels with CD31 staining.